HHS Public Access

Author manuscript

Nature. Author manuscript; available in PMC 2010 December 01.

Published in final edited form as:

Nature. 2010 June 24; 465(7301): 1097–1101. doi:10.1038/nature09095.

Small regulatory RNAs inhibit RNA Polymerase II during the elongation phase of transcription

Shouhong Guang[1], **Aaron F. Bochner**[1], **Kirk B. Burkhart**[1], **Nick Burton**[1], **Derek M. Pavelec**[2], and **Scott Kennedy**[1,2,3]

[1]Laboratory of Genetics, University of Wisconsin, Madison, Wisconsin 53706, USA

[2]Department of Pharmacology, University of Wisconsin, Madison, Wisconsin 53706, USA

Abstract

Eukaryotic cells express a wide variety of endogenous small regulatory RNAs that regulate heterochromatin formation, developmental timing, defense against parasitic nucleic acids, and genome rearrangement. Many small regulatory RNAs are thought to function in nuclei [1-2]. For instance, in plants and fungi siRNAs associate with nascent transcripts and direct chromatin and/or DNA modifications [1-2]. To further understand the biological roles of small regulatory RNAs, we conducted a genetic screen to identify factors required for RNA interference (RNAi) in *C. elegans* nuclei [3]. Here we show that *nrde-2* encodes an evolutionarily conserved protein that is required for small interfering (si)RNA-mediated silencing in nuclei. NRDE-2 associates with the Argonaute protein NRDE-3 within nuclei and is recruited by NRDE-3/siRNA complexes to nascent transcripts that have been targeted by RNAi. We find that nuclear-localized siRNAs direct a NRDE-2-dependent silencing of pre-mRNAs 3' to sites of RNAi, a NRDE-2-dependent accumulation of RNA Polymerase (RNAP) II at genomic loci targeted by RNAi, and NRDE-2-dependent decreases in RNAP II occupancy and RNAP II transcriptional activity 3' to sites of RNAi. These results define NRDE-2 as a component of the nuclear RNAi machinery and demonstrate that metazoan siRNAs can silence nuclear-localized RNAs co-transcriptionally. In addition, these results establish a novel mode of RNAP II regulation; siRNA-directed recruitment of NRDE factors that inhibit RNAP II during the elongation phase of transcription.

We previously described a forward genetic screen for factors required for RNA interference (RNAi) in *C. elegans* nuclei [3]. This screen identified the Argonaute (Ago) protein NRDE-3, which transports siRNAs from the cytoplasm to the nucleus [3]. Here we report that this

---

[3]To whom correspondence should be addressed. Correspondence and requests for materials should be addressed to S.K. (sgkennedy@wisc.edu).

Author Contributions. S.G. performed genetic screening, generated constructs, and contributed Figs. 1a, 2b-c, 3b, 3e, 4a, s2, s6, s7, and s9-12. A.B. mapped *nrde-2*, generated transgenic lines, and contributed Figs. 1c-d, s3, and s5. K.B. contributed Figs. 1b, s7, and s3. N.B. contributed to Figs. 3a and s7. D.P. contributed Fig. 2a. S.K. wrote the paper and contributed Figs. 2d, 3c-d, 4b-d, s1, s2, s13, and s14.

Supplementary information is linked to the online version of the paper at www.nature.com/nature. A figure (S1) summarizing the main result of this paper is available in supplementary information.

Author information. NRDE-2 accession number is NP_496209. Reprints and permissions information is available at www.nature.com/reprints. The authors declare no competing financial interests.

screen identified twenty-eight mutant alleles defining the gene nuclear RNAi defective-2 (*nrde-2*). *nrde-2* was required for RNAi processes within nuclei. For instance, wild-type *C. elegans* animals silence the nuclear-retained *pes-10::GFP* mRNA following exposure to dsRNA targeting this *pes-10::GFP* mRNA (GFP RNAi) [3,4]. *nrde-2* mutant animals failed to silence the *pes-10::GFP* mRNA following GFP RNAi, indicating that a wild-type copy of *nrde-2* is required for dsRNA-mediated silencing of this nuclear-localized RNA (Fig. 1a and Fig. S2). The *lin-15b* and *lin-15a* genes are expressed as a bicistronic RNA, which is separated into distinct *lin-15b* and *lin-15a* RNAs within the nucleus. Animals lacking both *lin-15b* and *lin-15a*, but not either gene product alone, exhibit a multi-vulva (Muv) phenotype [5,6]. RNAi targeting *lin-15b* alone is sufficient to induce a Muv phenotype, arguing that nuclear-localized *lin-15b/a* RNA can be silenced by RNAi [3]. *nrde-2(-)* animals failed to exhibit a Muv phenotype in response to *lin-15b* RNAi (Fig. 1b). Similarly, NRDE-2 was required for silencing the nuclear-localized *lir-1/lin-26* polycistronic RNA (Fig. 1b, and materials and methods). Thus, NRDE-2 is required for RNAi-based silencing of these nuclear-localized RNAs.

To determine the molecular identity of *nrde-2* we mapped *nrde-2* to a genetic interval containing the gene T01E8.5. Sequencing of T01E8.5 from six independent *nrde-2* mutant strains identified six mutations in T01E8.5 (Fig. 1c). Transformation of wild-type T01E8.5 DNA into *nrde-2* mutant animals rescued *nrde-2* mutant phenotypes (Fig. 1b). Thus, T01E8.5 corresponds to *nrde-2*. *nrde-2* encodes an ≈130 kDa protein (NRDE-2) containing a conserved domain of unknown function (DUF) 1740, and two domains frequently found in RNA processing factors; a serine/arginine (SR) rich domain, and half-a-tetratricopeptide (HAT)-like domains (Fig. 1c, and Fig. S3). A single putative orthologue of NRDE-2 was found in plant, fission yeast, insect, and mammalian genomes [7]. A fusion gene between GFP and NRDE-2 (GFP::NRDE-2), which was sufficient to rescue *nrde-2(-)* mutant phenotypes (Fig. 1b), localized predominantly to the nucleus (Fig. 1d). Finally, animals harboring putative null alleles of *nrde-2* produce ≈ 25% the number of progeny as wild-type animals (Fig. S4). We conclude that *nrde-2* encodes a conserved and nuclear-localized protein that is important for fecundity and is required for nuclear RNAi.

We sought to clarify the relationship between NRDE-2 and the Ago protein NRDE-3. Genetic analyses demonstrated that *nrde-2* and *nrde-3* function in the same genetic pathway (Fig. 2a). NRDE-2, however, was not required for NRDE-3 to transport siRNAs from the cytoplasm to the nucleus; NRDE-3 bound siRNAs, and in response to siRNA binding, localized to the nucleus similarly in both *nrde-2(+)* and *nrde-2(-)* animals (Fig. 2b). These data suggest that NRDE-2 may function downstream of NRDE-3-mediated siRNA transport during nuclear RNAi. In support of this hypothesis, we observed a weak, but reproducible, association between NRDE-3 and NRDE-2; NRDE-3 co-precipitated 0.1% to 0.5% of the total cellular pool of NRDE-2 (Fig. 2c). Conversely, NRDE-3 co-precipitated with NRDE-2 (Fig. S5). A NRDE-3 variant harboring mutations within its nuclear localization signal (termed NRDE-3(*NLS)) localizes constitutively to the cytoplasm [3]. NRDE-2 did not co-precipitate with NRDE-3(*NLS) (Fig. 2c). Taken together, these data argue that NRDE-2 functions downstream of NRDE-3/siRNA transport in the nuclear RNAi pathway and associates with NRDE-3 in the nucleus.

siRNAs direct NRDE-3 to bind pre-mRNAs that have been targeted by RNAi. For instance, following RNAi targeting *lir-1*, *unc-40*, or *dpy-28*, we detected a >200-fold increase in the amount of *lir-1*, *unc-40*, or *dpy-28* pre-mRNA that co-precipitated with NRDE-3, respectively (Fig. S6) [3]. The RNAi-directed association of NRDE-3 with pre-mRNA depends upon the ability of NRDE-3 to bind siRNAs and the ability of NRDE-3 to localize to the nucleus [3]. NRDE-2 was not required for NRDE-3 to associate with pre-mRNA: in *nrde-2(+)* and *nrde-2(-)* animals NRDE-3 was recruited to pre-mRNAs with similar efficiency (Fig. 2d). As *nrde-2(-)* animals are disabled for nuclear RNAi, these data indicate that the recruitment of NRDE-3/siRNA complexes to pre-mRNAs is not sufficient to trigger nuclear silencing. Interestingly, RNAi also directed NRDE-2 to pre-mRNAs; *lin-15b* RNAi induced a >300-fold increase in the amount of *lin-15b* pre-mRNA that co-precipitated with NRDE-2 (Fig. 2d). >10-fold less pre-mRNA co-precipitated with NRDE-2 in *nrde-3*(-) animals than in *nrde-3(+)* animals, indicating that RNAi directs NRDE-2 to pre-mRNAs in a largely NRDE-3 dependent manner (Fig. 2d). Similar results were obtained when an endogenous mRNA target of the NRDE pathway was analyzed (Fig. S7). Taken together, these data indicate that, following RNAi, NRDE-2 is recruited to pre-mRNAs by NRDE-3, which itself is localized to pre-mRNAs by siRNA/pre-mRNA base pairing.

In order to further our understanding of nuclear RNAi, we conducted a reverse genetic screen for nuclear RNAi factors (Fig. S8). This screen identified *nrde-2* and *nrde-3*, as well as five additional putative nuclear RNAi factors (Fig. S8). Rpb7 is a subunit of RNA Polymerase (RNAP) II that functions in siRNA-mediated heterochromatin formation in *S. Pombe* [8]. Our screen identified the *C. elegans* orthologue of Rpb7 (*rpb-7*); RNAi of *rpb-7* induced nuclear RNAi defects similar to those induced by RNAi of *nrde-2* or *nrde-3* (Fig. 3a, and Fig. S8). The identification and characterization of mutant alleles of *C. elegans rpb-7* will be required to confirm a role for *rpb-7* in *C. elegans* nuclear RNAi. Nonetheless, these data hint that nuclear RNAi may act concurrently with RNAP II transcription in *C. elegans*.

Five additional lines of investigation cumulatively argue that nuclear RNAi operates during the elongation phase of transcription. First, pre-mRNA splicing is thought to occur co-transcriptionally [9]. Therefore, the association of NRDE-2/3 with unspliced RNAs suggests that nuclear RNAi operates near or at the site of transcription (Fig. 2d). Second, we subjected animals undergoing RNAi to chromatin immunoprecipitation (ChIP) detecting tri-methylated (me3) H3K9 and found that RNAi directed a NRDE-2-dependent enrichment of H3K9me3 at a genomic site targeted by RNAi (Fig. 3b and Fig. S9). These data establish that, as in other organisms, *C. elegans* siRNAs direct H3K9 methylation, and support the idea that nuclear RNAi in *C. elegans* operates in close proximity to the site of transcription. Third, we isolated RNA from animals subjected to RNAi targeting *lin-15b*, *lir-1*, or *dpy-28* and measured pre-mRNA abundance at multiple sites distributed across the length of these pre-mRNAs, respectively. RNAi resulted in NRDE-2 dependent silencing of these pre-mRNAs 3' to the site of RNAi (Fig. 3c and Fig. S10). These data argue that nuclear RNAi is unlikely to occur at the initiation phase of transcription. Rather, these data argue that nuclear RNAi operates during transcription elongation. Incidentally, these data also show that, for unknown reasons, the relative contribution of the nuclear RNAi pathway to overall RNAi-

based silencing can vary, depending on the gene targeted by RNAi (Fig. S10c) [3]. Fourth, following bouts of *dpy-28* RNAi, NRDE-2 and NRDE-3 associated with *dpy-28* pre-mRNA fragments encoded upstream (5') of the site of RNAi with >200 fold greater efficacy than sequences encoded downstream (3') of the site of RNAi (Fig. 3d). Similar results were obtained following *lin-15b*, *lir-1*, and *unc-40* RNAi (Fig. S11). Nuclear silencing events were required for the preferential association of NRDE-3 with 5' pre-mRNA fragments; in *nrde-2(-)* animals, NRDE-3 associated with pre-mRNA sequences encoded both 5' and 3' to the site of RNAi with equal efficiency (Fig. S11c). These data support the idea that nuclear RNAi silences pre-mRNAs during the elongation phase of transcription, and suggest that NRDE-2/3 remain associated with pre-mRNA fragments following silencing. Fifth, we subjected animals undergoing RNAi to Chromatin Immunoprecipitation (ChIP) targeting the largest subunit of RNAP II, AMA-1/Rpb1. AMA-1/Rpb1 occupancy increased near genomic regions targeted by RNAi (Fig. 3e and Fig. S12). No changes in RNAP II occupancy were observed near sites of transcription initiation. Increases in AMA-1/Rpb1 occupancy were dependent upon NRDE-2; *nrde-2(-)* animals did not exhibit changes in AMA-1/Rpb1 occupancy following RNAi (Fig. 3e and Fig. S12). Thus, RNAi elicits NRDE-2-dependent increases in AMA-1/Rpb1 occupancy at or near genomic sites targeted by RNAi, arguing that siRNAs regulate RNAP II elongation. Taken together, these data indicate that *C. elegans* siRNAs, acting in conjunction with NRDE-2/3, silence nascent transcripts during the elongation phase of transcription.

Interestingly, we detected a decrease in AMA-1/Rpb1 occupancy downstream of the site of *lin-15b* (and to a lesser extent *lir-1*) RNAi, suggesting that siRNAs might inhibit RNAP II transcription (Fig. 3e and Fig. S12). Two additional lines of evidence support this hypothesis. First, we quantified *lin-15b* pre-mRNA associated with RNAP II before and after *lin-15b* RNAi. This effect was dependent upon NRDE-2, and was observed 3', but not 5', to the site of RNAi (Fig. 4a). Second, we established a *C. elegans* nuclear run-on assay utilizing 5-bromouridine 5'-triphosphate (Br-UTP). This approach detected *lin-15b* transcription, which was sensitive to the RNAP II inhibitor α-amanitin (Fig. 4b). *ama-1(m118m526)* encodes a mutant variant of AMA-1/Rbp1 that is resistant to α-amanitin [10]. Transcription from *ama-1(m118m526)* nuclei was insensitive to α-amanitin treatment (Fig. 4b). Finally, *lin-15b* transcription was not detected when reactions were carried out with nuclei harboring a *lin-15b* deletion allele (Fig. 4b). Thus, our nuclear run-on assay measures RNAP II-mediated transcription of the *lin-15b* locus. *lin-15b* RNAi induced a NRDE-2/3-dependent inhibition of RNAP II transcription 3' to the site of *lin-15b* RNAi (Fig. 4c and Fig. S13). siRNA-directed RNAP II inhibition was observed ≈ 2 kb downstream of the site of RNAi, hinting that (following recruitment of NRDE-2) additional molecular events may be required to silence RNAP II. Shifting the location of RNAi towards the 5' end of the *lin-15b* gene resulted in a coincident shift in patterns of RNAP II inhibition, indicating that the response of RNAP II to RNAi was sequence directed and sequence specific (Fig. S14). Finally, *lir-1* RNAi directed a similar NRDE-2-dependent inhibition of RNAP II transcription downstream of the site of *lir-1* RNAi (Fig. 4d). We conclude that siRNAs-direct a NRDE-2/3-dependent inhibition of RNAP II activity that occurs during the elongation phase of transcription. It should be noted that the decreases in RNAP II occupancy and RNAP II activity that we observe 3' to sites of RNAi argue that

siRNAs, acting in conjunction with NRDE-2/3, are likely to terminate RNAP II transcription.

Transcription is a highly regulated process. Here we describe a novel mechanism by which transcription can be regulated; small regulatory RNA-dependent recruitment of NRDE factors that inhibit RNAP II during the elongation phase of transcription. Eukaryotic cells express a multitude of small regulatory RNAs and antisense transcripts that are of unknown function. It will be of interest to test whether these RNAs regulate RNAP II via the mechanism described here. The mechanism of nuclear silencing in *C. elegans* is enigmatic. Many Ago proteins function via endonucleolytic cleavage of target RNAs (slicer activity) [11]. The Ago protein NRDE-3 lacks residues required for slicer activity, indicating that nuclear RNAi in *C. elegans* is unlikely to depend upon NRDE-3-mediated slicing of pre-mRNAs [3,12]. We have show that nuclear RNAi silences pre-mRNAs co-transcriptionally and that nuclear RNAi inhibits RNAP II elongation and transcription. Thus, our data suggest a mechanism for nuclear RNAi: siRNA-directed co-transcriptional silencing of RNAP II. Alternatively, the RNAP II inhibition we observe may represent a secondary consequence of another (currently unknown) co-transcriptional silencing activity associated with the Nrde pathway. Finally, NRDE-2 is directed to nascent transcripts by siRNAs and NRDE-2 is required for linking siRNAs to RNAP II inhibition. NRDE-2 is conserved. It will therefore be of interest to assess whether small regulatory RNAs and RNAP II are similarly linked in other metazoans.

Methods Summary

The following strains were used for this work. (YY151) *eri-1(mg366); nrde-2(gg091)*, (YY158) *nrde-3(gg066)*,(YY174) *ggIS1*[*nrde-3p*::*3xflag*::*gfp*::*nrde-3*], (YY178) *eri-1(mg366); ggIS1*, (YY186) *nrde-2 (gg091)*, (YY197) *nrde-2(gg091); axIs36*[*pes-10*::*gfp*], (YY229) *nrde-2(gg091); ggIS1*, (YY258) *nrde-2(gg091); nrde-3(gg066)*, (YY298) *nrde-3(gg066); ggIS24*[*nrde-3p*::*3xflag*::*gfp*::*nrde-3*nls*], (YY323) *eri-1(mg366); nrde-2(gg091); unc-119(ed3); ggIS28*[nrde-3p::3xflag::gfp::nrde-2], (YY346), *nrde-2(gg091); ggIS28*, (YY353) *nrde-2(gg091); ggIS1; ggIS36*[*nrde-3p*::*3xha*::*gfp*::*nrde-2*], (YY363) *nrde-3(gg066); nrde-2(gg091); ggIS28*, (GR1373) *eri-1(mg366)*, (wm27) *rde-1(ne219)*, (DR1099) *ama-1(m118m526)*, (MT309) *lin-15AB(n309)*, (JH103) *axIs36*. Worm culture conditions, plasmid construction, feeding RNAi assay, *lir-1* RNAi assay, RNA *in situ* hybridization, fluorescence imaging, cDNA preparation, NRDE-2/3 co-precipitation, RNA immunoprecipitation (RIP), RNA isolation, quantitative real time PCR, chromatin immunoprecipitation (ChIP), and nuclear run-on (NRO) assays are described in detail in Methods.

Supplementary Material

Refer to Web version on PubMed Central for supplementary material.

Acknowledgments

We thank Phil Anderson, members of the Anderson lab, David Wassarman, and David Brow for comments, and the *Caenorhabditis* Genetics Center (CGC) for strains. This work was supported by grants from the PEW and Shaw scholars programs, the NIH, and the AHA.

References

1. Matzke MA, Birchler JA. RNAi-mediated pathways in the nucleus. Nat Rev Genet. 2005; 6(1):24–35. [PubMed: 15630419]
2. Moazed D. Small RNAs in transcriptional gene silencing and genome defence. Nature. 2009; 457(7228):413–20. [PubMed: 19158787]
3. Guang S, Bochner AF, Pavelec DM, et al. An Argonaute transports siRNAs from the cytoplasm to the nucleus. Science. 2008; 321(5888):537–41. [PubMed: 18653886]
4. Montgomery MK, Xu S, Fire A. RNA as a target of double-stranded RNA-mediated genetic interference in *Caenorhabditis elegans*. Proc Natl Acad Sci U S A. 1998; 95(26):15502–7. [PubMed: 9860998]
5. Clark SG, Lu X, Horvitz HR. The *Caenorhabditis elegans* locus lin-15, a negative regulator of a tyrosine kinase signaling pathway, encodes two different proteins. Genetics. 1994; 137(4):987–97. [PubMed: 7982579]
6. Huang LS, Tzou P, Sternberg PW. The lin-15 locus encodes two negative regulators of *Caenorhabditis elegans* vulval development. Mol Biol Cell. 1994; 5(4):395–411. [PubMed: 8054684]
7. Tatusov RL, Fedorova ND, Jackson JD, et al. The COG database: an updated version includes eukaryotes. BMC Bioinformatics. 2003; 4:41–55. [PubMed: 12969510]
8. Djupedal I, Portoso M, Spahr H, et al. RNA Pol II subunit Rpb7 promotes centromeric transcription and RNAi-directed chromatin silencing. Genes & Development. 2005; 19(19):2301–6. [PubMed: 16204182]
9. Moore MJ, Proudfoot NJ. Pre-mRNA processing reaches back to transcription and ahead to translation. Cell. 2009; 136(4):688–700. [PubMed: 19239889]
10. Rogalski TM, Golomb M, Riddle DL. Mutant *Caenorhabditis elegans* RNA polymerase II with a 20,000-fold reduced sensitivity to alpha-amanitin. Genetics. 1990; 126(4):889–98. [PubMed: 2076819]
11. Liu J, Carmell MA, Rivas FV, et al. Argonaute2 is the catalytic engine of mammalian RNAi. Science. 2004; 305(5689):1437–41. [PubMed: 15284456]
12. Yigit E, Batista PJ, Bei Y, et al. Analysis of the *C. elegans* Argonaute family reveals that distinct Argonautes act sequentially during RNAi. Cell. 2006; 127(4):747–57. [PubMed: 17110334]
13. Duchaine TF, Wohlschlegel JA, Kennedy S, et al. Functional proteomics reveals the biochemical niche of *C. elegans* DCR-1 in multiple small-RNA-mediated pathways. Cell. 2006; 124(2):343–54. [PubMed: 16439208]
14. Lee RC, Hammell CM, Ambros V. Interacting endogenous and exogenous RNAi pathways in *Caenorhabditis elegans*. RNA. 2006; 12(4):589–97. [PubMed: 16489184]

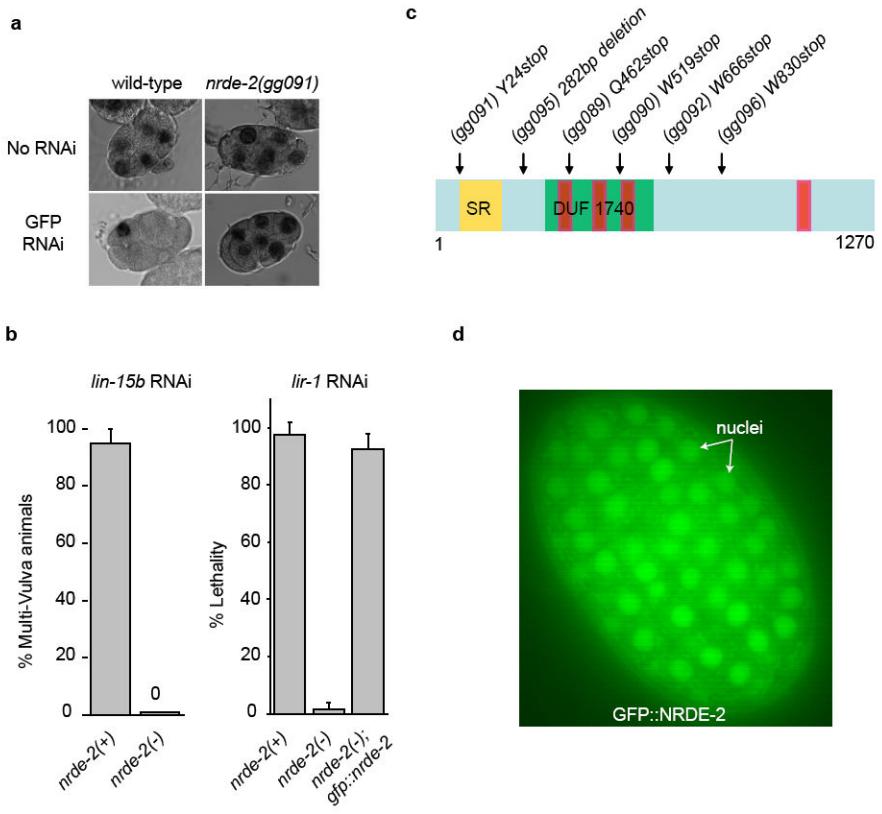

Figure 1. *nrde-2* encodes a conserved and nuclear-localized protein that is required for nuclear RNAi

(a) Light microscopy of ≈6-cell embryos +/- GFP RNAi subjected to *in situ* hybridization detecting *pes-10:: gfp* RNA. **(b)** *nrde-2(-)* animals fail to silence the *lin-15b/lin15a* and *lir-1/lin-26* nuclear-localized RNAs (n=4, +/- s.d.). An *eri-1(-)* genetic background was used for this analysis **(c)** Predicted domain structure of NRDE-2. (Yellow) SR domain. (Green) DUF1740. (Red) potential HAT-like repeats. **(d)** Fluorescent microscopy of a ≈200 cell embryo expressing a rescuing GFP:: NRDE-2 fusion protein.

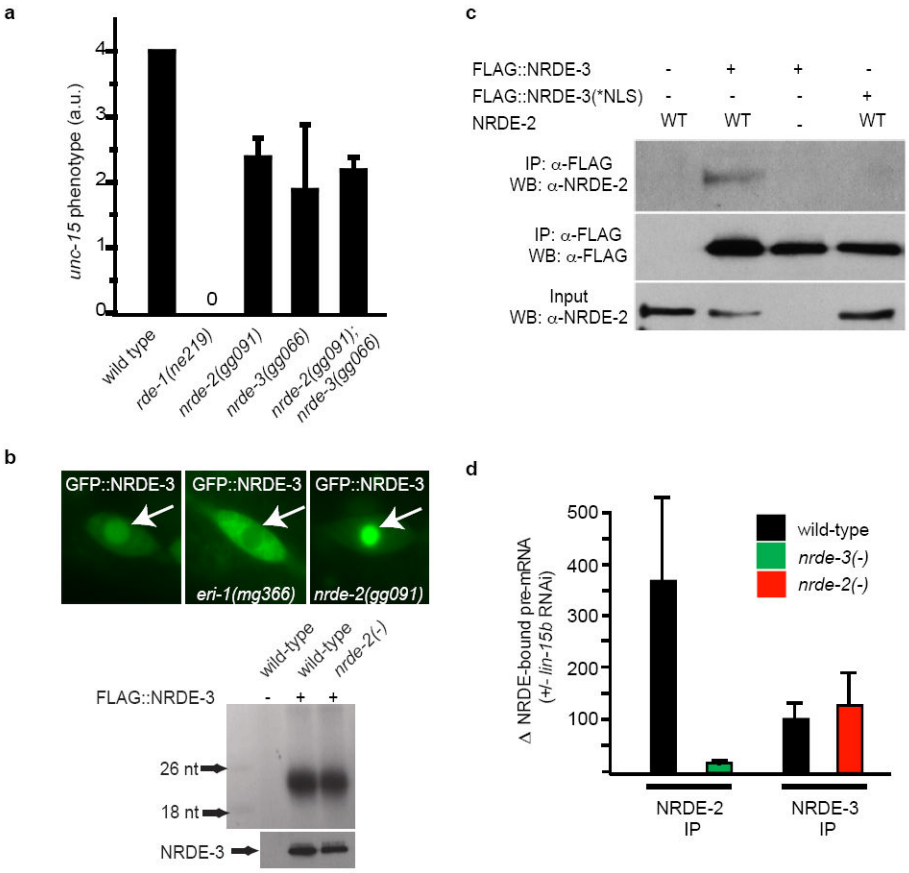

Figure 2. NRDE-2 is recruited by NRDE-3/siRNA complexes to pre-mRNAs that have been targeted by RNAi

(a) Animals were exposed to *unc-15* dsRNA and scored for uncoordinated phenotypes (Unc) (n=3, +/- s.d.). *rde-1(ne219)* animals are defective for RNAi [12]. **(b)** (top panels) Fluorescent microscopy of a seam cell expressing GFP: :NRDE-3. Arrows indicate nuclei. *eri-1(mg366)* animals fail to express endo siRNAs and consequently NRDE-3 is mislocalized to the cytoplasm [3,13,14]. (bottom panels) FLAG: :NRDE-3 co-precipitating RNAs ^{32}P-radiolabeled and analyzed by PAGE. **(c)** NRDE-2 co-precipitates with nuclear-localized NRDE-3 (materials and methods) (n=3). **(d)** qRT-PCR quantification of NRDE-2/3 co-precipitating pre-mRNA. Throughout this manuscript pre-mRNA levels are quantified with exon/intron or intron/intron primer pairs. Data are expressed as ratios of co-precipitating pre-mRNA +/- *lin-15b* RNAi (n=4 for NRDE-2 IP, n=2 for NRDE-3 IP, +/- s.e.m.). Δ=fold change.

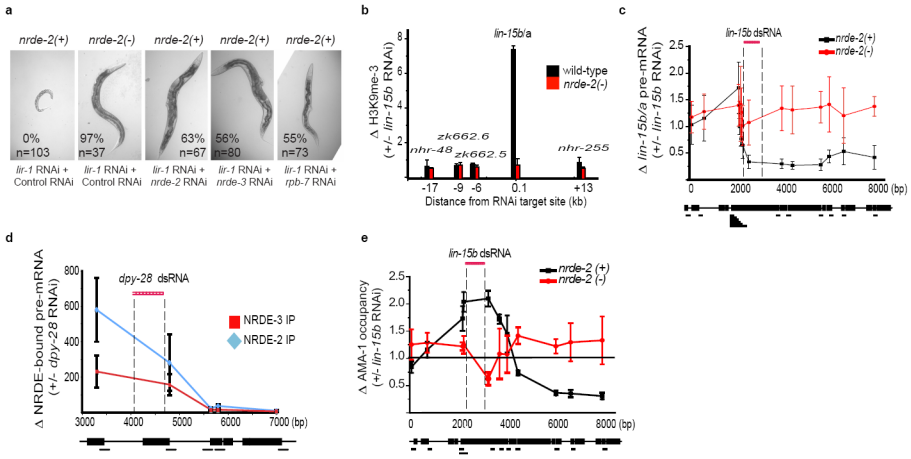

Figure 3. *C. elegans* siRNAs direct a NRDE-2/3-dependent co-transcriptional gene silencing program

(a) Animals were exposed to one part *lir-1* dsRNA expressing bacteria and 6 parts vector control, *nrde-2/3*, or *rpb-7* dsRNA expressing bacteria. (%) indicates percentage of animals that failed to exhibit *lir-1* RNAi phenotypes. **(b)** Chromatin IP with H3K9me3 antibody (Upstate, #07-523). Data are expressed as ratio of H3K9me3 co-precipitating DNA +/- *lin-15b* RNAi, (n=2). **(c)** Total RNA was isolated and *lin-15b* pre-mRNA was quantified with qRT-PCR. Data are expressed as ratios +/- *lin-15b* RNAi. (**c**) and (**e**) were done in an *eri-1(-)* genetic background. **(d)** FLAG: :NRDE-2/3 co-precipitating *dpy-28* pre-mRNA. Data are expressed as ratio +/- *dpy-28* RNAi (n=4, +/- s.d.). **(e)** Chromatin IP of AMA-1/ Rpb1 with α-AMA-1 antibody (Covance, 8WG16). Data are expressed as ratio of AMA-1 co-precipitating DNA +/- *lin-15b* RNAi (n=3, +/- s.d.).

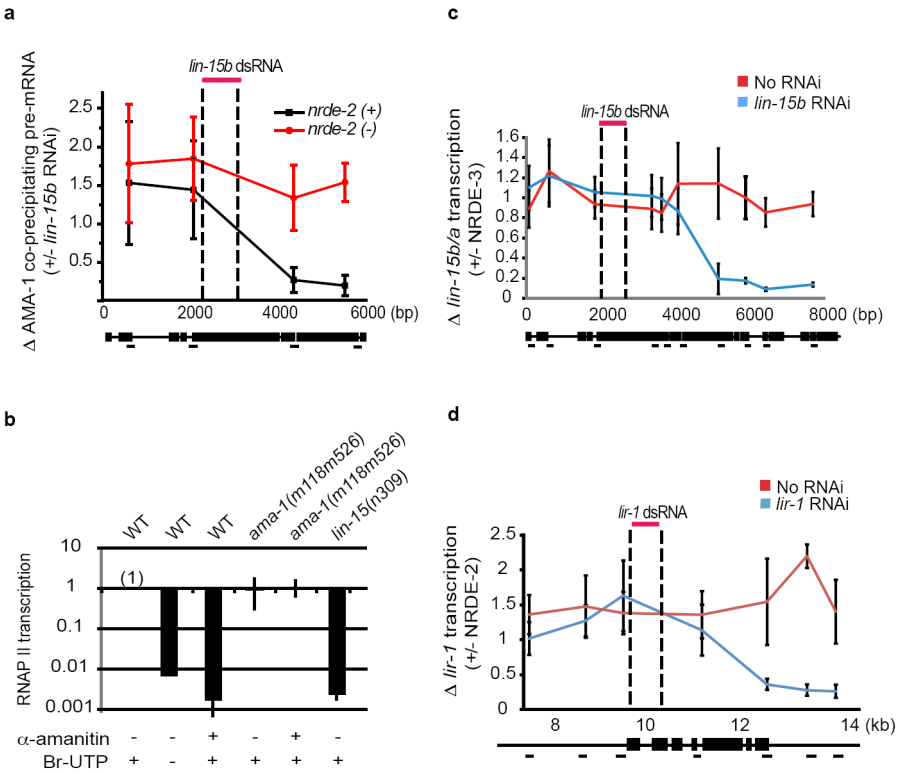

Figure 4. siRNAs direct a NRDE-2/3-dependent inhibition of RNAP II during the elongation phase of transcription

(a) AMA-1 co-precipitating pre-mRNA. Data are expressed as ratio +/- *lin-15b* RNAi (n=3, +/- s.d.). **(b)** A crude preparation of nuclei was subjected to nuclear run-on analysis (see materials and methods). Transcription detected from wild-type (WT) nuclei was defined as one (n=3, +/- s.d.). **(c-d)** RNAi inhibits RNAP II activity 3' to sites of RNAi. An *eri-1(-)* genetic background was used for these analyses. Nuclei isolated from animals treated with *lin-15b* **(c)** or *lir-1* **(d)** RNAi were subjected to run-on analysis. Data are expressed as ratio of transcription detected in *nrde-3(+)/nrde-3(-)* nuclei **(c)** or *nrde-2(+)/nrde-2(-)* nuclei **(d)** (n=5, for **c**, and n=3 for **d**, +/- s.e.m.).